Paramagnetic Meissner effect from the self-consistent solution of the Ginzburg-Landau equations

V. V. Moshchalkov, X. G. Qiu,* and V. Bruyndoncx
Laboratorium voor Vaste-Stoffysica en Magnetisme, Katholieke Universiteit Leuven, Celestijnenlaan 200D, B-3001 Leuven, Belgium
(Received 1 March 1996)

The paramagnetic Meissner effect (PME), recently observed in high-T_c materials and also in Nb, can be successfully explained by the persistence of a giant vortex state with a fixed orbital quantum number L. This state is formed in superconductors in the field-cooled regime at the third critical field. The self-consistent numerical solution of the Ginzburg-Landau equations clearly shows that the compression of the flux trapped inside the giant vortex state can result in the PME. The PME is suppressed, and the normal diamagnetic response is recovered, by increasing the applied field. A possible definition of the irreversibility line, as a crossover between the giant vortex state and the Abrikosov flux line lattice, is discussed. The transition between the two quantum states ($L=0$ and $L=1$) has been used to calculate the field $H_{0\to1}(T)$, corresponding to the penetration of the first flux line into a cylindrical sample. [S0163-1829(97)03317-1]

I. INTRODUCTION

The most characteristic features of a superconductor are zero resistivity (infinite or ''super'' conductivity) and strong diamagnetic response (Meissner-Ochsenfeld effect) below the superconducting transition temperature T_c. In superconductors with a weak flux line pinning, a perfect *diamagnetic* state can be reached in the so-called field-cooled (FC) regime, when a superconductor is cooled down in a certain applied magnetic field. Recently, an enigmatic *paramagnetic Meissner effect* (PME) has been found in high-T_c granular materials, such as $Bi_2Sr_2CaCu_2O$,[1–7] and then in a few $YBa_2Cu_3O_7$ single crystals[8] for the FC magnetization measurements. A detailed systematic study of this effect has been carried out by the Wohlleben group in Cologne, and afterwards the PME has often been referred to as the ''Wohlleben effect.''[9] The PME is usually observed as a very strong (up to 60% of $1/4\pi$) paramagnetic FC response in relatively low fields of the order of 0.1–1 G. Later on, the anomalous PME has been interpreted in the framework of different models, such as spontaneous currents due to the presence of π contacts,[6,10–12] vortex pair fluctuations combined with pinning,[1] d-wave superconductivity,[9] orbital glass,[13] and Josephson junctions.[14]

The recent observation of the PME in niobium disks by Thompson *et al.* and Kostic *et al.*,[15] however, indicates that the PME can also occur in conventional low-T_c superconductors and it may be related to flux trapping. In 1992 one of the authors of the present paper[16] suggested that the PME can be caused by the persistence of the giant vortex state with the fixed orbital quantum number $L>0$. This state is formed in any finite-size superconductor in the FC regime at the third (surface) critical field H_{c3}. The superconducting order parameter $\Psi=|\Psi|e^{L\phi}$, nucleated at the sample surface, traps then inside, in the sample interior, a giant vortex,[17] carrying flux $L\Phi_0$ where Φ_0 is the flux quantum. Crossing the H-T plane by lowering the temperature at constant field, the order parameter at the sample boundary, corresponding to $L>1$, grows and it compresses the flux $L\Phi_0$ trapped inside the sample at $H_{c3}(T)$. This flux compression may eventually lead to the onset of the paramagnetic response.

To check this ''flux compression'' model quantitatively, the self-consistent solution of the full Ginzburg-Landau (GL) equations is necessary, though the phase boundary $H_{c3}(T)$ itself can be found just by solving the linearized GL equation.

In what follows in Sec. II, we first consider the formation of the giant vortex state at $H_{c3}(T)$ by solving the linearized first GL equation for a long cylinder in a parallel field. Then, in Sec. III, we proceed to the numerical self-consistent solution of the two GL equations below the $H_{c3}(T)$ boundary. We demonstrate that the PME can indeed be obtained in the FC model if the orbital momentum L is kept constant. The stability of the giant vortex state $L=$const with respect to its decay into conventional Abrikosov vortex lattice (with one flux quantum Φ_0 per vortex) is also briefly discussed in this section. In Sec. IV we describe another interesting case: the zero-field-cooled (ZFC) regime of the magnetization measurements. We show that the magnetic response in this case can be found assuming that the order parameter, corresponding to the state with $L=0$, is realized. Along similar line, in Sec. IV, we will calculate the first critical field $H_{c1}(T)$, if to interpret it, in its literal sense, as a temperature-dependent transition field $H_{0\to1}(T)$ between the $L=0$ and $L=1$ quantum states. Finally, we conclude with a summary of the major new results.

II. NUCLEATION OF THE SUPERCONDUCTING PHASE

The nucleation of the superconducting phase is usually analyzed in the framework of the linearized GL equation for the superconducting order parameter Ψ:[18]

$$\frac{1}{2m}\left(-i\hbar\vec{\nabla}-\frac{e^*}{c}\vec{A}\right)^2\Psi=-\alpha\Psi, \tag{1}$$

which is identical to the Schrödinger equation for a particle with charge $e^*=2e$ in a uniform magnetic field given via the vector potential $H=\nabla\times A$ with $E=-\alpha$. The parameter $-\alpha$ in the GL equation thus plays the role of energy E in the Schrödinger equation:

$$E=-\alpha=\frac{\hbar^2}{2m\xi^2(T)}=\frac{\hbar^2}{2m\xi^2(0)}\frac{T_{c0}-T}{T_{c0}}. \tag{2}$$

Here $\xi(T)$ is the temperature-dependent coherence length, T is the actual temperature, and T_{c0} is the critical temperature at zero magnetic field.

In finite superconducting samples the order parameter Ψ obeys the boundary condition for a superconductor-insulator interface:[18]

$$\left(-i\hbar\overline{\nabla}-\frac{e^*\overline{A}}{c}\right)\Psi|_n=0. \tag{3}$$

This boundary condition is quite different from the normal boundary condition in the quantum mechanical problem ''particle in a box,'' where the density $\Psi\Psi^*$ is zero at the boundary.

As a result of the relation between E and α [Eq. (2)], we have to follow a simple rule: solve the Schrödinger equation with proper boundary conditions [Eq. (3)] and take the lowest energy $E(H)$ which gives the highest T in Eq. (2), coinciding with the phase boundary $T_{c3}(H)$ for the nucleation of the superconducting state.

The important point here is the role of the boundary conditions [Eq. (3)]. In large bulk samples the lowest Landau level with $E=\hbar\omega/2$ (here ω is the cyclotron frequency) gives the upper critical field H_{c2}:

$$H_{c2}(T)=\frac{\hbar c}{e^*\xi^2(0)}\frac{T_{c0}-T}{T_{c0}}=\frac{\Phi_0}{2\pi\xi^2(T)}. \tag{4}$$

In small samples, however, the surface-to-volume ratio is large and boundary conditions [Eq. (3)] must be taken into account. The crucial question is, what is a small sample? To answer this question we may refer again to the analogy between the Schrödinger equation for normal electrons and the linearized GL equation for the superconducting order parameter Ψ. The former was used by Dingle[19] in connection with the analysis of quantum oscillations in small metallic samples. Though Dingle took different boundary conditions, we expect that his conclusions are also valid for the ''superconducting'' boundary conditions. According to Dingle, the border between small and large samples can be found from the estimate

$$H\times r_0\approx 5(\text{G cm}), \tag{5}$$

based on the coincidence between the Larmor radius r_L and the sample radius r_0. If the product of field H times disk radius r_0 is smaller than 5 G cm (or $r_0<r_L$), then boundary conditions essentially modify the solution of Eq. (1). It is evident that fields $H<5$ (G cm)$/r_0$ are not extremely low. Indeed, for a sample with dimensions, say, 1 mm, the field below which boundary conditions should be taken into account is 50 G. In this context we use the word ''small'' in this section. First, we shall analyze the onset of the superconducting state in small long cylindrical samples in a parallel field. The demagnetizing effects for this particular geometry are negligible. The boundary conditions [Eq. (3)] will be taken into account explicitly.

The description of the superconducting state in long cylinders in a parallel field should be based on the choice of an adequate system of coordinates. Apparently, the sample symmetry implies the choice of the cylindrical coordinates (r,ϕ,z) and the gauge $A=(Hr/2)\overline{e_\phi}$, where $\overline{e_\phi}$ is the tangential unit vector. The solution of the Hamiltonian [Eq. (1)] in cylindrical coordinates has the form[20]

$$\Psi(r,\phi)=e^{\pm iL\phi}r^L\gamma^{(L+1)/2}\exp\left(-\frac{\gamma r^2}{2}\right)M(-N,L+1,\gamma r^2). \tag{6}$$

Here $\gamma=e^*H/(2\hbar c)$ and the energy $E_\perp$ of the motion in the plane perpendicular to H is determined by the orbital quantum number L and parameter N, which is not necessarily an integer number, as we shall see later:

$$E_\perp=\frac{e^*\hbar H}{2mc}(2N\pm L+L+1). \tag{7}$$

The function M is the Kummer function defined as

$$M(a,c,y)=1+\frac{a}{c}y+\frac{a(a+1)}{c(c+1)}\frac{y^2}{2!}+\frac{a(a+1)(a+2)}{c(c+1)(c+2)}\frac{y^3}{3!}+\cdots, \tag{8}$$

where $a=-N$, $c=L+1$, and $y=\gamma r^2$. Introducing the dimensionless radius $R=\sqrt{\gamma}r$, the superconducting order parameter can be written in the form

$$\Psi_L(R,\phi)=e^{\pm iL\phi}R^L\exp\left(-\frac{R^2}{2}\right)M(-N,L+1,R^2). \tag{9}$$

The representation of the order parameter $\Psi=\Sigma_L c_L\Psi_L$ as an expansion over states with different L for *infinite* samples has been analyzed in Ref. 21, where $M(0,L+1,R^2)=1$ has been taken. Under these conditions, the functions $|\Psi_L|$ have their maxima at $R^2=L$; i.e., the area enclosed by the circle with the radius corresponding to the $|\Psi_L|$ maximum is always penetrated by an integer number L of the flux quanta: $\Phi/\Phi_0=L$. Here in this paper we shall analyze the case of *finite* samples, where the N value has to be found from the boundary condition [Eq. (3)]. It is very important to note that in the general form [Eqs. (6) and (7)] there are no limitations on the parameter N: It is not necessarily an integer number. The only argument, which is usually given in favor of taking integer N, is a possibility to get a cut off in the summation [Eq. (8)]. Indeed, if we insert an integer N into the summation, then by adding 1 to N in each new term we shall eventually come to the situation where $-N+N=0$ and all subsequent terms in the summation will be equal to zero. Thus by the cutoff we just use a finite number of terms in the summation [Eq. (8)], and of course M is finite in this case. But we should keep in mind that any converging row also gives a finite solution for M. Therefore, not only the positive integer N in Eq. (7), but also noninteger and even negative N values are possible. In finite-size samples the N value, which we further denote as $N(L,R_0)$, has to be found from the boundary condition at $R=R_0$ [Eq. (3)], where R_0 is the normalized disk radius:

$$\left.\frac{\partial|\Psi(R)|}{\partial R}\right|_{R=R_0}=0. \tag{10}$$

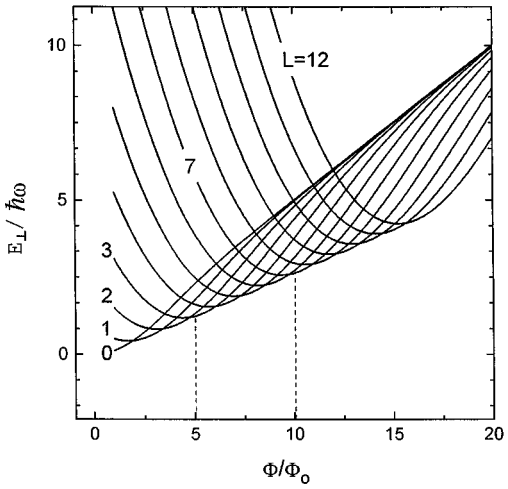

FIG. 1. Energy $E_\perp$ vs normalized flux Φ/Φ_0 for a superconducting cylinder in a parallel magnetic field. The vertical dashed lines illustrate which orbital quantum number L is fixed at $H_{c3}(T)$ in the FC mode; for example, $L=3$ for $\Phi/\Phi_0=5$ and $L=7$ for $\Phi/\Phi_0=10$.

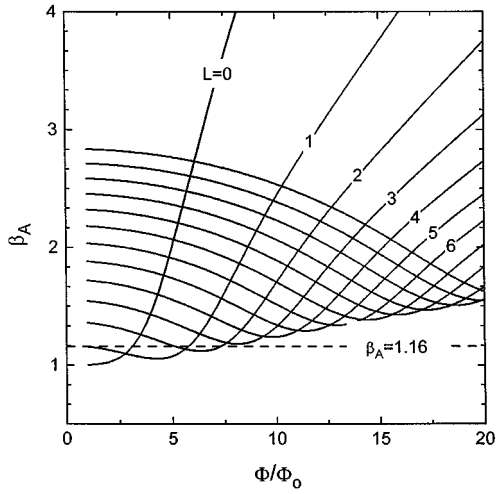

FIG. 2. Field dependence of the Abrikosov parameter β_A for different orbital quantum momenta L.

Since we are looking for the lowest possible energy state, we should take the minus sign in the argument of the exponent $\exp(-iL\phi)$ in the solution given by Eq. (6). In this case $-L$ and $+L$ in Eq. (7) cancel, and for any L the energy levels become

$$E_\perp=\hbar\omega(N+\tfrac{1}{2}), \tag{11}$$

where $\omega=e^*H/mc$ is the cyclotron frequency.

This result coincides with the well-known Landau quantization, but now *N is any real number, including negative real number*, which is to be calculated from Eq. (10). Using the expression

$$\frac{dM(a,c,y)}{dy}=\frac{a}{c}\,M(a+1,c+1,y)$$

for the derivative of the Kummer function, we can find the $N(L,R_0)$ value, which obeys the boundary condition [Eq. (10)], from the equation

$$(L-R_0^2)M(-N,L+1,R_0^2)-\frac{2NR_0^2}{L+1}\,M(-N+1,L+2,R_0^2)=0. \tag{12}$$

The remarkable thing about the $N(L,R_0)$ values, found from the solutions of Eq. (12), is that they are negative which immediately gives the energy $E_\perp$ in Eq. (11) lower than $\hbar\omega/2$. *As a result of the confinement with the ''superconducting'' boundary conditions, the energy levels in finite samples lie below the classical value $\hbar\omega/2$ for infinite samples.*[22,23] The whole energy level scheme (Fig. 1), found by Saint-James,[22] can be reconstructed by calculating $E_\perp$ vs R_0^2 for different L values. From this diagram we can easily go to the ''field versus temperature'' plot, using the relation $E_\perp=-\alpha$. The corresponding values of the Abrikosov parameter β_A, giving an idea about the ''flatness'' of $|\Psi|$,[25] are plotted in Fig. 2. It should be noted that β_A for certain L and H (see the levels below the dashed line in Fig. 2) is smaller than the well-known minimum possible value $\beta_A=1.16$ for the triangular Abrikosov vortex lattice.

To conclude this section, we note that in finite samples N is a bad ''quantum number.'' It is rather a parameter which has to be found from the boundary condition. A ''good quantum number'' for the problem is L. By forming a superconducting condensate with a proper finite L and $N(L,R_0)<0$, we conserve the rotational momentum and at the same time reduce the energy below $\hbar\omega/2$.

As shown above, because of the onset of the surface superconductivity at $H_{c3}(T)$, corresponding to negative N in Eq. (11), the superconductivity can appear well above the $H_{c2}(T)$ line (found for $N=0$). By changing the variable $E_\perp$ in Fig. 1 into T, we obtain the cusplike phase boundary $H_{c3}(T)$ as shown in Fig. 3, which is due to switching between different orbital momenta L. The phase boundary of the superconducting disk (Fig. 3) has been observed experimentally by Buisson *et al.*[23] and by Moshchalkov *et al.*[24] The linear component of the cusplike $H_{c3}(T)$ line is $1.695H_{c2}$, which is in good agreement with the calculations of H_{c3} in the $L\to\infty$ limit.[18]

III. PARAMAGNETIC MEISSNER EFFECT

By cooling down a superconductor in a fixed applied field (FC mode), we are crossing the $H_{c3}(T)$ boundary at a particular point corresponding to a certain orbital quantum number L (see horizontal dashed lines in Fig. 3). The phase boundary $H_{c3}(T)$ is calculated in this case from the linearized GL equation with boundary conditions being properly taken into account as shown above. Below $H_{c3}(T)$, however, the solution of the full GL equations is necessary, since a nucleating superconducting condensate creates its own additional magnetic field which should be treated self-consistently.

In the following, a similar cylindrical geometry as in the last section will be considered. The starting point for our calculation is the system of two coupled GL equations which reads in dimensionless form as[25]

$$\left(\frac{1}{i\kappa}\,\overline{\nabla}-\overline{A}\right)^2\Psi=\Psi(1-|\Psi|^2), \tag{13}$$

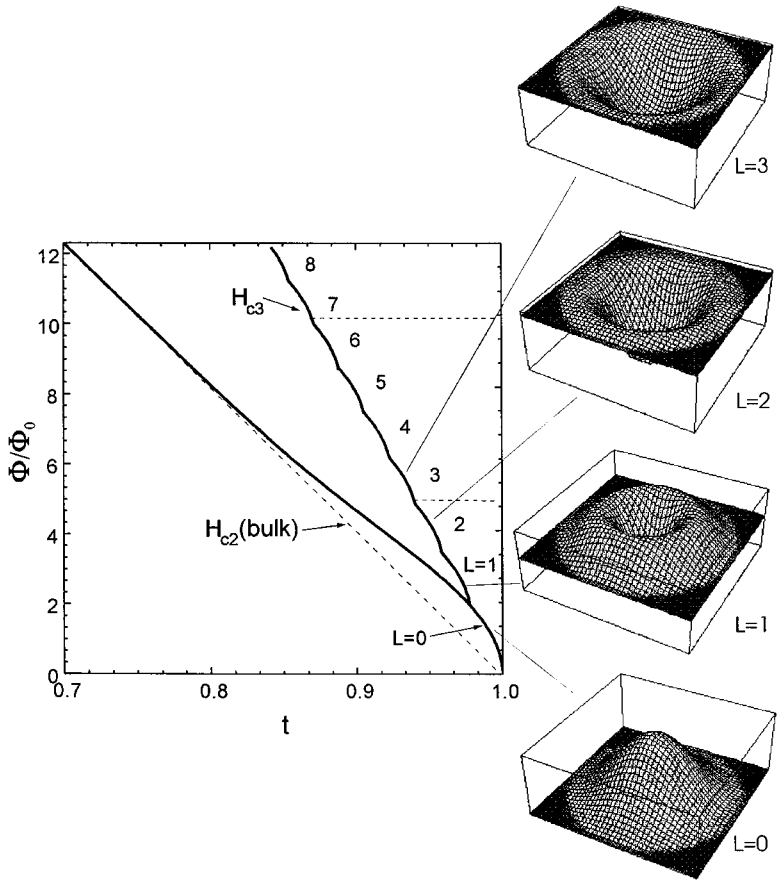

FIG. 3. Third critical field H_{c3} and the bulk upper critical field H_{c2} (dashed line) vs normalized temperature $t=T/T_c$. The cusplike $H_{c3}(T)$ line is formed due to the change of the orbital quantum number L. In the three-dimensional plots, $|\Psi|$ is depicted as a function of the spatial coordinates for several L values.

$$\overline{\nabla}\times\overline{\nabla}\times\overline{A}=\frac{1}{2}\left\{\Psi^*\left[\frac{1}{i\kappa}\overline{\nabla}-\overline{A}\right]\Psi+\Psi\left[-\frac{1}{i\kappa}\overline{\nabla}-\overline{A}\right]\Psi^*\right\}, \tag{14}$$

where Ψ, $\overline{A}$, b, and r are in units of Ψ_∞, $\sqrt{2}H_c\lambda(0)$, $\sqrt{2}H_c$, and $\lambda(0)$, respectively, and $t=T/T_c$ is the reduced temperature. Ψ_∞, H_c, $\lambda(0)$, and κ are the wave function in bulk, the thermodynamical critical field, the penetration depth at zero field and zero temperature, and the GL parameter, respectively. We use the simplifications.

$$\Psi(r,\phi)=F(r)e^{iL\phi},\quad A=\frac{1}{2}Hr+\frac{1}{2}\frac{\varphi}{r},\quad b=H+\frac{1}{2r}\frac{d\varphi}{dr}. \tag{15}$$

H is the applied magnetic field which is in the z direction (in units of $\sqrt{2}H_c$), while b is the local induction given by the vector potential $\nabla\times A=b$. The function φ is to be determined. Inserting the above equations into Eqs. (13) and (14), taking into account the temperature dependence of Ψ which is given by $\Psi^2(t)=\Psi^2(0)(1-t)$, we get the two coupled equations[17]

$$\frac{d^2F}{dr^2}=-\frac{1}{r}\frac{dF}{dr}+\left(\frac{1}{2}\kappa Hr+\frac{1}{2}\frac{\kappa\varphi}{r}-\frac{L}{r}\right)^2F-\kappa F(1-F^2), \tag{16}$$

$$\frac{d^2\varphi}{dr^2}=\frac{1}{r}\frac{d\varphi}{dr}+\left(Hr^2+\varphi-\frac{2L}{\kappa}\right)F^2. \tag{17}$$

The corresponding boundary conditions for the above equations are,[17] at $r=r_0$

$$dF/dr=0,\quad d\varphi/dr=0 \tag{18}$$

and, at $r=0$,

$$\varphi=0,\quad F=0\quad \text{for } L\neq 0, \tag{19a}$$

$$dF/dr=0\quad \text{for } L=0. \tag{19b}$$

In the calculation given below, we have fixed the size of our sample at $r_0=\sqrt{3}\lambda(0)$.

The magnetization per unit volume $4\pi M$ is defined as

$$\frac{4\pi M}{H_c}=2\int_0^{r_0}r(b-H)dr=\varphi(r_0). \tag{20}$$

The difference of the Gibbs free energy between the superconducting (G_S) and normal (G_N) states is

$$\Delta g=\frac{G_S-G_N}{H_c^2V/2\pi}=\frac{1}{2}\int_0^{r_0}[(b-H)^2-F^4]r\,dr. \tag{21}$$

Using a numerical procedure, we have performed self-consistent calculations of the radial dependence of the normalized order parameter $F(r)=|\Psi|/|\Psi_0|$ [Figs. 4(a) and 5(a)], the function $\varphi(r)$ [Figs. 4(b) and 5(b)], and the local induction $b(r)$ [Figs. 4(c) and 5(a)] for fixed L and different normalized temperatures $t=T/T_c$, using the formalism described earlier in this section.

Following Fink and Presson,[17] we have assumed in these calculations that the orbital quantum number L, found according to the location of the crossing point between $H_{c3}(T)$ and $H=$const (Figs. 1 and 3), is kept constant also below the

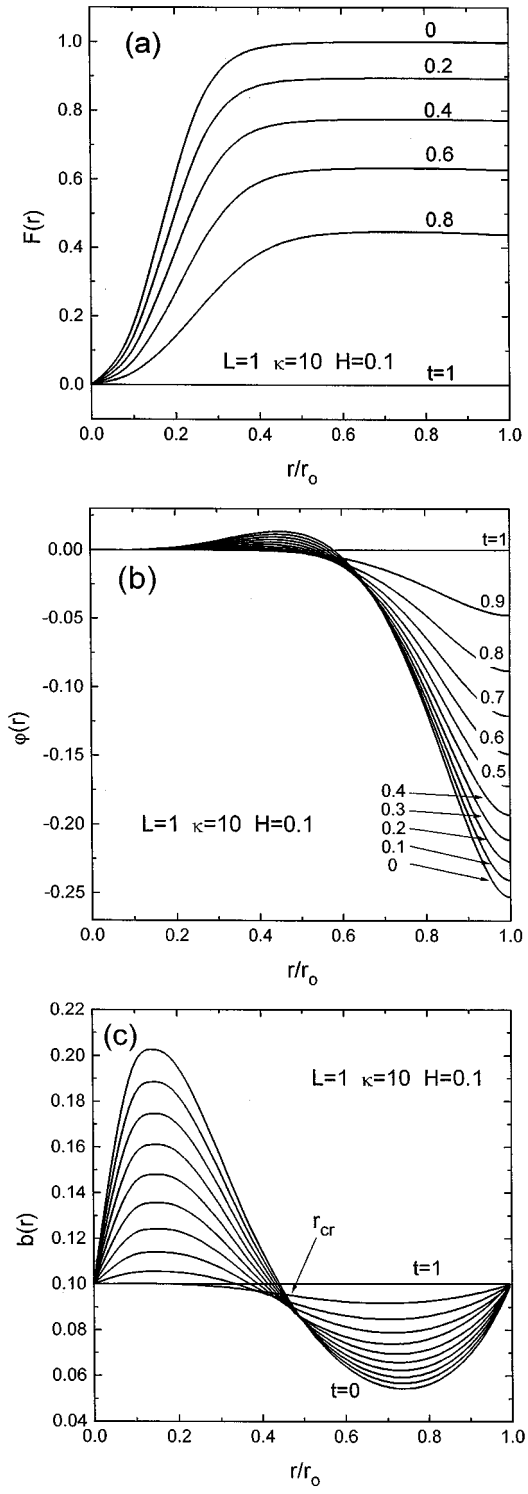

FIG. 4. Radial-dependent part of the order parameter $F(r)$ [Eq. (16)] (a), function $\varphi(r)$ [Eq. (15)] (b), and local induction $b(r)$ (c), calculated from Eqs. (16)–(19) for a superconductor with $\kappa=10$, fixed $L=1$ in a magnetic field $H=0.1$.

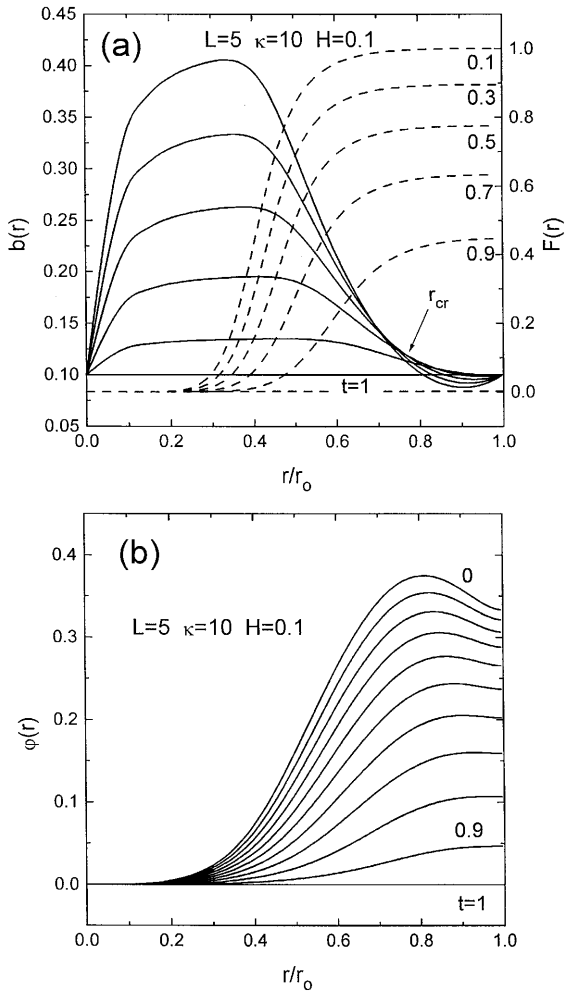

FIG. 5. Local induction $b(r)$ [Eq. (15)], radial-dependent part of the order parameter $F(r)$ [Eq. (16)] (a), and function $\varphi(r)$ [Eq. (15)] (b), calculated for $L=5$, $\kappa=10$, and $H=0$ for different normalized temperatures $t=T/T_c$.

$H_{c3}(T)$ line. The conservation of the orbital quantum number L in the superconducting state can result from pinning of the giant vortex state, corresponding to a ringlike superconducting order parameter nucleated at the sample boundary at $H_{c3}(T)$ (Fig. 3). The sample boundary itself pins the giant vortex state in this case. The conserved value $L=$const is determined by the applied field. For sufficiently small fields, the state with $L=1$ is realized. The normalized order parameter $F(r)$, calculated for this particular value of L [Fig. 4(a)], has a normal core penetrated by the flux line carrying one flux quantum Φ_0.

As temperature decreases, the $F(r)$ value grows and the London limit $|\Psi|=$const is recovered everywhere except in the vortex core area [see Fig. 4(a)]. As a result of the $F(r)$ increase, the trapped $L=$const vortex is compressed and this leads to an enhancement of $\varphi(r)$ [Fig. 4(b)] and $b(r)$ [Fig. 4(c)] in the core area of the sample interior and to a reduction of $\varphi(r)$ and $b(r)$ at the sample periphery. Similar behavior of $\varphi(r)$ and $b(r)$ is found for $L=5$, as shown in Figs. 5(a) and 5(b). The crossover point r_{cr} separating the areas, where $b(r)$ is enhanced or reduced, is L dependent, for example, for $L=1$ [see Fig. 4(c)] $r_{cr}\approx 0.40 r_0$, whereas for $L=5$ [see Fig. 5(a)], $r_{cr}\approx 0.75 r_0$.

From the calculated difference in Gibbs functions, Δg, between normal and superconducting states [Figs. 6(a) and 6(b)], it is evident that the conservation of the trapped orbital momentum ($L=$const) does not correspond to the lowest energy. At the same time, for superconductors with high κ [compare Fig. 6(a), $\kappa=10$, with Fig. 6(b), $\kappa=5$] the differ-

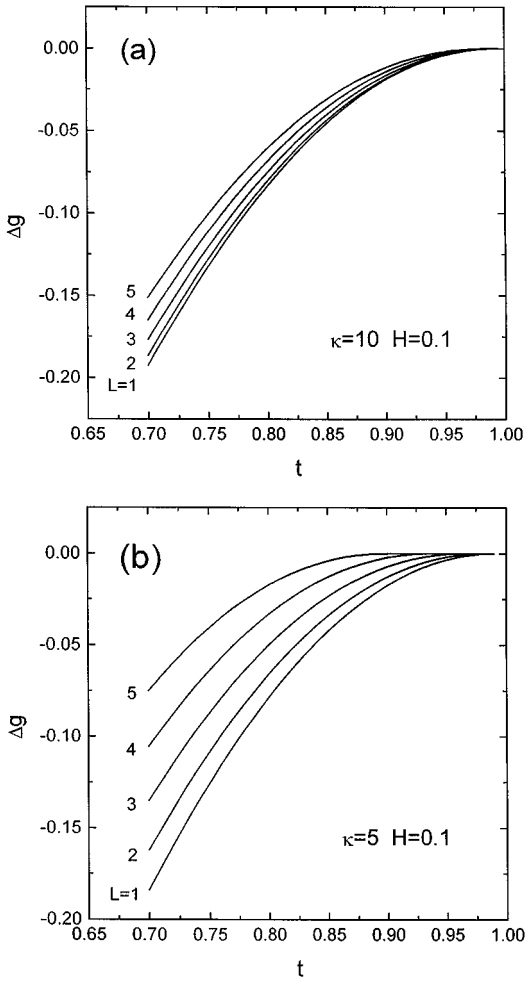

FIG. 6. Difference in the Gibbs potentials between superconducting and normal state [Eq. (21)] vs normalized temperature $t=T/T_c$ in magnetic field $H=0.1$ for a superconductor with GL parameter $\kappa=10$ (a) and $\kappa=5$ (b).

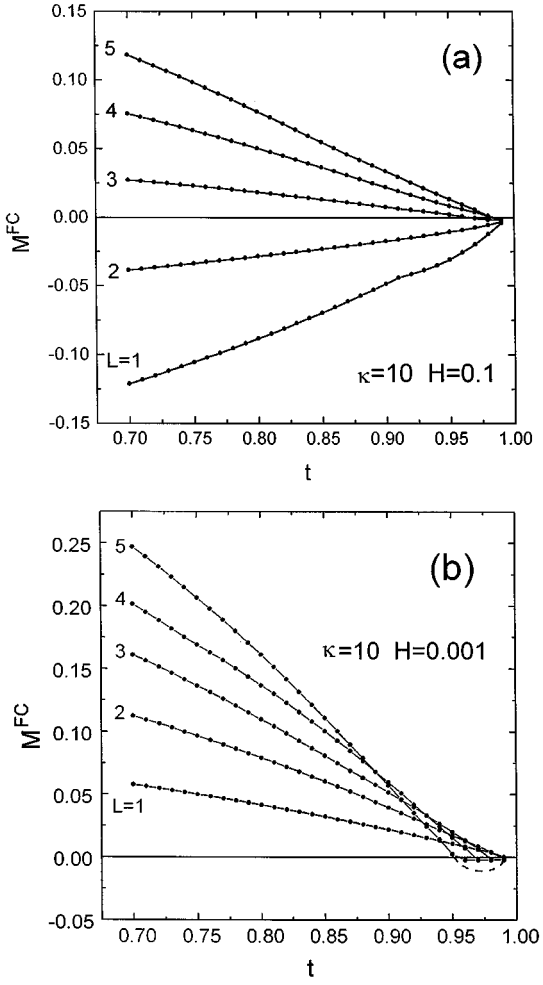

FIG. 7. Temperature dependence of the field cooled magnetization M^{FC} [Eq. (20)] of a superconductor with GL parameter $\kappa=10$ for different fixed orbital quantum momenta L in applied magnetic field $H=0.1$ (a) and $H=0.001$ (b).

ence between various $\Delta g(L)$ becomes very small. Taking this factor into account, as well as possible pinning of the giant vortex state itself, we can assume that in certain experimental conditions the tendency to conserve L may override the lowest-energy condition.

For $L=5$ [Fig. 5(a)] the vortex core and the area, where additional field $b(r)$ is generated due to the flux compression, are considerably larger than for $L=1$ [Fig. 4(a)]. Initially, at $L=5$ and $t=1$, $b(r)$ is constant through the sample and $|\Psi|=0$. As the temperature goes down, the order parameter grows and pushes the magnetic field into the core. It is clearly seen from our calculations [Figs. 4(a), 4(c), and 5(a)] that for the trapped $L\geqslant 1$ vortex the field $b(r)$ is localized in the area where the superconducting order parameter is strongly reduced. This reflects a very general flux expulsion property of a superconductor which causes either normal diamagnetic Meissner effect with complete flux expulsion for the state $L=0$ without a core or flux compression (PME) in the vortex core for $L\geqslant 1$. Topologically, $L=0$ and $L>0$ states are qualitatively different, since for the latter flux is expelled both inwards and outwards. When the former dominates, PME can appear. By separating the areas where the field penetrates from the ones where the order parameter nucleates, a kind of a ''peaceful coexistence'' of the two antagonistic phenomena—magnetism and superconductivity—becomes possible.

By integrating the radial-dependent induction $b(r)$, the magnetization $M=(B-H)/4\pi$ can be easily calculated. B is here the macroscopic induction. In fact [see Eq. (20) and Figs. 4(b) and 5(b)], the magnetization is given by $\varphi(r)$ at the sample boundary. In full agreement with the abovementioned expectation, the growth with decreasing temperature of the superconducting order parameter with a fixed orbital quantum number L results in the appearance of the PME [Figs. 7(a) and 7(b)].

The amplitude of the PME and the slope dM^{FC}/dt [see Fig. 7(b)] are dependent on L and are also very sensitive to the variation of the applied field. Indeed, for $H=0.1$ [Fig. 7(a)], only states with $L\geqslant 3$ demonstrate PME, whereas for a lower field $H=0.001$ all states with $L\geqslant 3$ exhibit the PME [Fig. 7(b)]. Fixing, for example, $L=2$ or $L=1$, and increasing the applied magnetic field from $H=0.001$ to $H=0.1$, the sign of the magnetic response can be changed from anomalous paramagnetic [$L=2$, $L=1$ in Fig. 7(a)] to conventional diamagnetic [$L=2$, $L=1$ in Fig. 7(b)]. This field suppression of the PME is in qualitative agreement with experiments

which have demonstrated that the anomalous PME can be observed only in weak field.[2–8]

Another interesting feature of the $M(T)$ curves related to the $L=$const states is a possibility to obtain the $M(T)$ sign inversion at temperatures very close to T_c. Indeed, the energy level pattern (Fig. 1), used to find the $H_{c3}(T)$ boundary (Fig. 3), is such that in the FC mode the crossing point between $H=$const and $H_{c3}(T)$ always corresponds to a smaller $L(H_{c3})$ than the one just calculated from the applied normalized flux $\Phi/\Phi_0=\pi r_0^2 H/\Phi_0$. For example, the $H_{c3}(T)$ segment, crossed by the $H=$const line for $\Phi/\Phi_0=5$ (Fig. 1), is given by the $E(L=3,H)$ level, for $\Phi/\Phi_0=10$, by the $E(L=7,H)$ level, etc. The difference $\Delta L=\Phi/\Phi_0-L(H_{c3})$ between the normalized applied flux Φ/Φ_0 and the particular $L(H_{c3})$ value resulting in the lowest-energy sublevel implies the diamagnetic response at temperatures just below $H_{c3}(T)$ line and very close to it.

The ''diamagnetic'' difference between these L's has already been discussed by de la Cruz *et al.*[26] who calculated the sign inversion of $M(T,H)$ in the vicinity of T_c. For large $L(H_{c3})$ values they found that

$$\frac{\Phi}{\Phi_0}-L(H_{c3})\approx\frac{R}{\xi_3(H)}, \tag{22}$$

where ξ_3 is the value of $\xi(T)$ at the crossing point between the $H_{c3}(T)$ line and the line $H=$const. The algorithm we were using for numerical calculations of Eqs. (16) and (17) was not very reliable for the calculation of the M^{FC} with the sign change at temperatures very close to T_c. Nevertheless, we have obtained a weak diamagnetic response at $T\to T_c$. Taking into account previous calculations,[17] we suggest that the kink at the $M^{\mathrm{FC}}(L=5,t)$ curve in Fig. 7(b) at $T\to T_c$ may be an artifact, and therefore in reality the $M^{\mathrm{FC}}(L=5,t)$ may eventually demonstrate a more pronounced sign inversion [see the dashed line in Fig. 7(b)], analyzed earlier in Ref. 26.

Summarizing this section, we would like to emphasize that the PME effect can be obtained from the self-consistent solution of the GL equations assuming that orbital quantum number L is conserved. In this case, the PME effect and its field dependence can be reproduced in the framework of a very simple and natural approach without making any further assumptions, related to the presence of a π junction[6,10–12] or d-wave superconductivity.[9] From this point of view, the recent observation of the PME in Nb disks[15] is not very surprising. The reported sensitivity to the surface treatment [15,27] may be caused by violation of the L conservation and recovery of a normal diamagnetic response corresponding to a transition from large L values trapped at H_{c3} to the state with $L=0$.

The PME is saturated at a certain temperature T_{sat}, which decreases with applied field.[2,6,8,15] Below T_{sat}, $M(T,H)$ curves are nearly temperature independent, thus forming an extended plateau. The crossover between $M(T,H)$ growing with decreasing temperature in the interval $T_{\mathrm{sat}}<T<T_c$ and the $M(T,H)$ plateau at $T<T_{\mathrm{sat}}$ is very sharp in single crystals[8] and may be interpreted as a consequence of an ''explosion'' of the giant vortex state with a core carrying flux $L\Phi_0$ into a collection of Abrikosov vortices, each carrying a flux Φ_0. From this point of view, the characteristic crossover temperature T_{sat} can be found by equating the Gibbs potentials for the Abrikosov vortex lattice and the giant vortex state. As was demonstrated by Fink and Presson,[17] the value for T_{sat}, obtained from this equation, is very sensitive to κ, applied field H, and sample size r_0. For example, for large samples and $\kappa>1.5$ the temperature T_{sat} corresponds to the crossing point between $H_{c2}(T)$ and $H=$const lines. For smaller samples the giant vortex state can be observed in fields even below $H_{c2}(T)$, quite close to $0.84\,H_{c2}(T)$.[17]

Let us assume now that inside a superconductor there are no pinning centers with the size comparable to the giant vortex core. In this case a giant vortex state is stabilized only by the sample surface and this state is reversible as long as the orbital quantum number L is kept constant. But as the temperature goes down, the multiquanta vortex state is assumed to decay rather quickly into Φ_0 vortices once the conservation of L is violated. As soon as the Abrikosov vortex lattice is formed ($T<T_{\mathrm{sat}}$), pinning centers, which are relatively small in comparison to the giant core, can be quite efficient to pin the Φ_0 vortices, thus leading to the onset of irreversibility. The irreversibility should then be considered as the consequence of the onset of the variation of L, initiating the crossover between the giant vortex state ($L=$const) and the Abrikosov vortex state ($L=1$) which should occur around the $H_{c2}(T)$ line. In other words, in superconducting samples where the surface pinning plays the dominant role in stabilizing the giant vortex state the irreversibility line $H_{\mathrm{irr}}(T)$ seems to lie in fact, quite close to the upper critical field $H_{c2}(T)$.

On the other hand, if a superconducting sample contains imperfections, impurities, etc., preventing the formation of the equilibrium $F(r)$ distribution found from the self-consistent solution of the GL equations [see Figs. 4(a) and 5(a)], then the equilibrium $F(r)$ and $b(r)$ profiles can only be reached after a certain relaxation time. This delay in the formation of the equilibrium $b(r)$ and $F(r)$ states for changing fields and/or temperatures may result in flux creep phenomena. It is worth mentioning here that magnetization can increase or decrease, depending on the specific shape of the equilibrium $b(r)$ distribution, which the system tends to reach. The unusual logarithmic increase of magnetization has indeed been observed experimentally.[7]

IV. TRANSITION BETWEEN $L=0$ AND $L=1$ STATES

States with orbital quantum numbers $L>0$ correspond to the rotation of the superconducting condensate caused by the action of the Lorentz force, when an external magnetic field is applied to a superconducting sample. If the sample is cooled down through T_c in zero magnetic field, then it seems reasonable to expect that superconducting state with $L=0$ is formed. Using the self-consistent solution of the GL equations for $L=0$, we can calculate the ZFC magnetization $M^{\mathrm{ZFC}}(T,H)$ for different fields H applied already in the superconducting state $T<T_c$ with $L=0$.

The results of these calculations are shown in Fig. 8. We clearly see the dependence of magnetization $M^{\mathrm{ZFC}}(T\to 0,H)$ upon applied magnetic field, which agrees qualitatively with measurements of the superconducting transition in the ZFC mode in different fields.

As a next step, we consider the onset of flux penetration into a superconducting film as the transition between the two quantum states: $L=0$ and $L=1$. This transition defines actu-

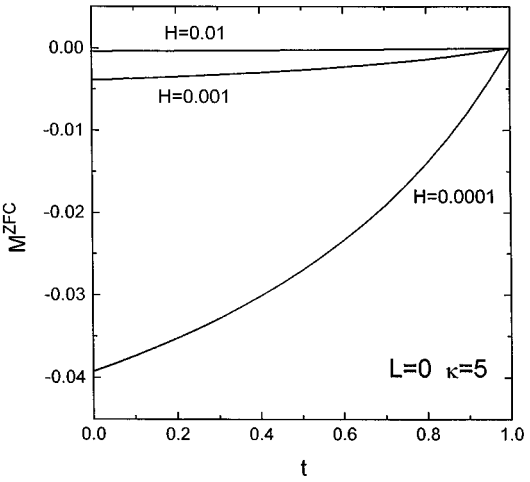

FIG. 8. Temperature dependences of magnetization M^{ZFC} in the zero-field-cooled mode for different applied fields.

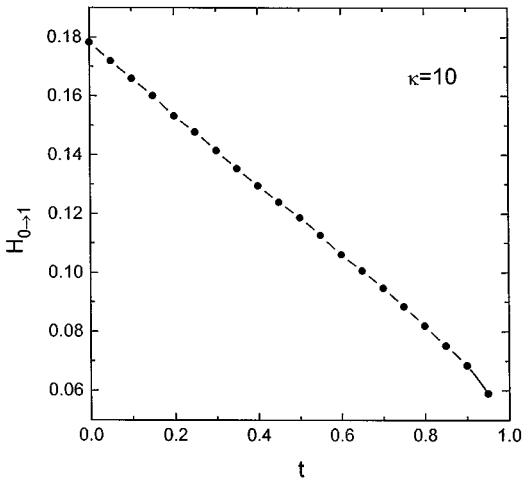

FIG. 9. Temperature dependence of the crossover field $H_{0\to1}$ between the two quantum states $L=0$ and $L=1$.

ally the lower critical field $H_{c1}(T)$, if one treats the definition ''the onset of penetration'' really as a penetration of the first flux quantum into a sample. To avoid confusion, however, we use the notation $H_{0\to1}$ instead of the conventional H_{c1}. The transition between $L=0$ and $L=1$ states occurs if the Gibbs energy for the latter is lower than for the former. Using again numerical self-consistent solution of the GL equations, we have determined the field $H_{0\to1}$ for different temperatures (Fig. 9). The $H_{0\to1}(T)$ curve shows linear dependence $H_{0\to1}(T)\propto 1-T/T_c$ for low temperatures and a square-root behavior $H_{0\to1}(T)\propto(1-T/T_c)^{1/2}$ at $T\to T_c$.

We think that the field $H_{0\to1}(T)$ can be used to analyze experimental data on $H_{c1}(T)$ if these data were measured with a superconducting quantum interference device (SQUID), having a very low threshold for the registration of the onset of the flux penetration. We may also argue that linear H_{c1} vs T dependence often seen in high-T_c cuprates at low temperatures (see, for example, Ref. 28) can be interpreted simply as the intrinsic behavior of $H_{0\to1}(T)$, taking into account the sensitive methods used in Ref. 28 to determine the H_{c1} values.

V. CONCLUSION

In conclusion, we would like to emphasize that the main result, obtained in this paper, is an interpretation of the enigmatic PME observed recently in high-T_c superconductors and also in Nb. In our approach we did not use any sufficiently sophisticated model to interpret the available experimental data on the PME. Instead, we have solved the GL equations self-consistently for a fixed orbital quantum number L and found that the PME can be caused by the compression of the flux L, which is trapped inside a superconducting sample below the third (surface) critical field $H_{c3}(T)$, when the sample magnetization is measured in a field-cooled mode. A similar flux compression mechanism of the PME has been recently considered by Koshelev and Larkin.[29] We have demonstrated that the amplitude of the PME is suppressed by applying a magnetic field. A possible definition of the irreversibility line as a crossover line between the giant vortex state and Abrikosov flux lattice has been given. The transition between the two quantum states ($L=0$ and $L=1$) has been used to calculate the field corresponding to the penetration of one flux line at different temperatures. Finally, we would like to note that our explanation of the PME in terms of the conventional GL equations does not exclude, of course, other possible explanations.[1,6,10–12] At the same time, our model should not be omitted before making any final conclusion concerning the nature of the PME in superconductors.

ACKNOWLEDGMENTS

The authors are thankful to Y. Bruynseraede for useful discussions. This work is supported by the Flemish Concerted Action (GOA), the Belgian Inter-University Attraction Poles (UIAP), the Fund for Scientific Research (FWO) Programs, and the European INTAS-94-3562 Project.

*Present address: Research Laboratory of Engineering Materials, Tokyo Institute of Technology, Japan.

[1] P. Svedlindh, K. Niskanen, P. Norling, P. Nordblad, L. Lundgren, B. Lönnberg, and T. Lundström, Physica C **162-164**, 1365 (1989).

[2] W. Braunisch, N. Knauf, V. Kataev, S. Neuhausen, A. Grütz, B. Roden, D. Khomskii, and D. Wohlleben, Phys. Rev. Lett. **68**, 1908 (1992).

[3] B. Schliege, M. Stindtmann, I. Nikolic, and K. Baberschke, Phys. Rev. B **47**, 8331 (1993).

[4] Ch. Heinzel, Th. Theiling, and P. Zieman, Phys. Rev. B **48**, 3445 (1993).

[5] S. Elschner, J. Bock, and H. Bestgen, Supercond. Sci. Technol. **6**, 413 (1993).

[6] W. Braunisch, N. Knauf, G. Bauer, A. Kock, A. Becker, B. Freitag, A. Grüz, V. Kataev, S. Neuhausen, B. Roden, D. Khomskii, D. Wohlleben, J. Bock, and J. Preisler, Phys. Rev. B **48**, 4030 (1993).

[7] J. Magnusson, M. Björnander, L. Pust, P. Svedlindh, P. Nordblad, and T. Lundström, Phys. Rev. B **52**, 7675 (1995).

[8] S. Riedling, G. Bräuchle, R. Lucht, K. Röhberg, H. v. Löhneysen, H. Claus, A. Erb, and G. Müller-Vogt, Phys. Rev. B **49**, 13 283 (1994).
[9] M. Sigrist and T. M. Rice, J. Phys. Soc. Jpn. **61**, 4283 (1992).
[10] D. Dominguez, E. A. Jagla, and C. A. Balseiro, Phys. Rev. Lett. **72**, 2773 (1994).
[11] D.-X. Chen and A. Hernando, Europhys. Lett. **26**, 365 (1994).
[12] D. Khomskii, J. Low Temp. Phys. **95**, 205 (1994).
[13] F. V. Kusmartsev, Phys. Rev. Lett. **69**, 2268 (1992).
[14] K. N. Shrivastava, Solid State Commun. **90**, 589 (1994); Phys. Lett. A **188**, 182 (1994).
[15] D. J. Thompson, M. S. M. Minhaj, L. E. Wenger, and J. T. Chen, Phys. Rev. Lett. **75**, 529 (1995); P. Kostic, B. Veal, A. P. Paulikas, U. Welp, V. R. Todt, C. Gu, U. Geiser, J. M. Wiliams, K. D. Carlson, and R. A. Klemm, Phys. Rev. B **53**, 791 (1996).
[16] V. V. Moshchalkov (unpublished).
[17] H. J. Fink and A. G. Presson, Phys. Rev. **151**, 219 (1966).
[18] P. G. de Gennes, *Superconductivity of Metals and Alloys* (Addison-Wesley, New York, 1966).
[19] R. B. Dingle, Proc. R. Soc. London, Ser. A **212**, 47 (1952).
[20] R. B. Dingle, Proc. R. Soc. London, Ser. A **211**, 500 (1952).
[21] V. V. Moshchalkov, M. Dhallé, and Y. Bruynseraede, Physica C **207**, 307 (1993).
[22] D. Saint-James, Phys. Lett. **15**, 13 (1965).
[23] O. Buisson, P. Gandit, R. Rammal, Y. Y. Wang, and B. Pannetier, Phys. Lett. A **150**, 36 (1990).
[24] V. V. Moshchalkov, L. Gielen, C. Strunk, R. Jonckheere, X. Qiu, C. Van Haesendonck, and Y. Bruynseraede, Nature **373**, 319 (1995).
[25] A. A. Abrikosov, *Fundamentals of the Theory of Metals* (North-Holland, Amsterdam, 1988).
[26] F. de la Cruz, H. J. Fink, and J. Luzuriaga, Phys. Rev. B **20**, 1947 (1979).
[27] R. Lucht, H. v. Löhneysen, H. Claus, M. Kläser, and G. Müller-Vogt, Phys. Rev. B **52**, 9724 (1995).
[28] V. V. Moshchalkov, C. Marin, J. Y. Henry, J. Rossat-Mignod, and J. F. Jacquot, Physica C **175**, 407 (1991).
[29] A. E. Koshelev and A. I. Larkin, Phys. Rev. B **52**, 13 559 (1995).